SUPPLEMENTAL MATERIAL

Supplemental Methods

Processing and Visualization of Images from Fixed Tissue. The three-dimensional image stacks were corrected for background signals and depth-dependent attenuation.[1, 2] We applied the Richardson-Lucy algorithm based on measured point spread functions (PSFs) to deconvolve the image stacks. 3D volume visualizations of exemplary image stacks of AWM, SAN, and AVN were produced using VolView (Kitware, Inc. Clifton Park, New York). The depth of the epicardial tissue layer was detected from the WGA associated signal. WGA signal intensity from XY images was averaged along the z-direction for samples of AWM, SAN and AVN tissue. The maximal increase and decrease of averaged WGA signal served as a marker of the start and end of an epicardial layer. The depth of nodal tissue was detected from the HCN4 associated signal using a similar approach. The maximal increase and decrease of averaged HCN4 signal served as a marker of the start and end of a nodal tissue layer.

Signal-To-Noise Ratio (SNR). The SNR was calculated from image sequences of SAN regions labeled with dextran conjugated Alexa Fluor 488 and acquired with a fiber-optics confocal microscope. SNR is defined as the ratio between the mean of the signal and the standard deviation of the signal. In our case, regions of interest (ROI) of approximately 700 pixels were selected that represented an area of high signal intensity and an area of low signal intensity for each image sequence. These high and low intensity areas corresponded to regions with both signal and noise-only regions, respectively. An average SNR was determined based on background corrected image sequences. Image sequences with an SNR below two deviations of the average SNR were excluded from Fourier and image moment analyses

Quantitative Analysis of HCN4 Signal Intensity. Signal and background intensities were measured from acquired images of fluorescent dye solutions excited with the 543 nm laser line. We sampled those intensities in a range of laser powers, gains, and pixel dwell times. A three-dimensional calibration curve was calculated based on the measured mean intensities for the imaged solution with respect to the sampled laser powers, gains, and pixel dwell times. The AWM, nodal and subnodal layers were determined based on WGA and HCN4 depth profiles generated from image stacks of rat AWM (n = 7/4), SAN (n = 5/4), and AVN (n = 6/3). Sample size n is denoted as $n = I/A$ with I = images and A = animals. The HCN4 mean intensities from these layers were corrected based on the established calibration curve in a similar manner as we corrected depth dependent attenuation.

References

1. Lackey DP, Carruth ED, Lasher RA, Boenisch J, Sachse FB, Hitchcock RW. Three-dimensional modeling and quantitative analysis of gap junction distributions in cardiac tissue. *Ann. Biomed. Eng.* 2011;39:2683-2694
2. Lasher RA, Hitchcock RW, Sachse FB. Towards modeling of cardiac micro-structure with catheter-based confocal microscopy: A novel approach for dye delivery and tissue characterization. *IEEE Trans Med Imaging*. 2009;28:1156-1164

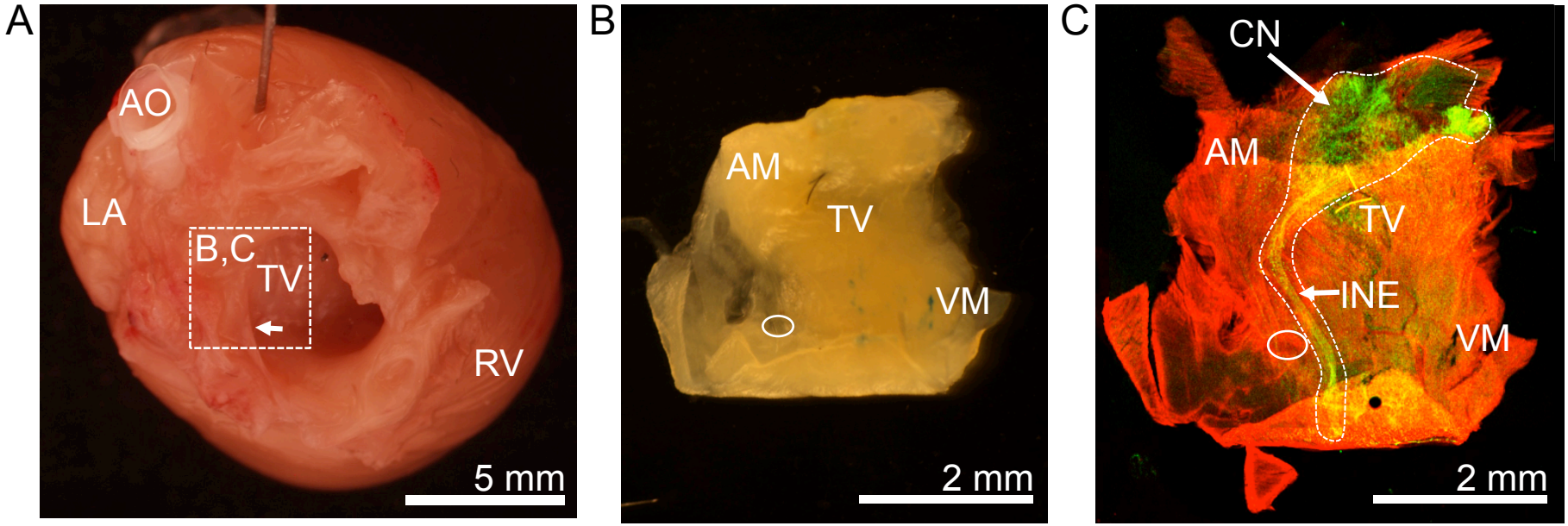

Supplemental Figure 1. Preparation for localization and characterization of AVN tissue. (**A**) Fixed rat heart with right atrial lateral wall and right atrial appendage removed shown from cranial. Arrow indicates location of coronary sinus. (**B**) Tissue section from region marked in (**A**). (**C**) Conventional confocal microscopic image of tissue preparation in (**B**) labeled for anti-HCN4 (**green**) and anti-sarcomeric α-actinin (**red**). HCN4-positive regions were outlined region. Circle in (**B,C**) marks location of coronary sinus. AM, atrial muscle; AO, aorta; CN, compact node; INE, inferior nodal extension; LA, left atrium, RV, right ventricle; TV, tricuspid valve; VM, ventricular muscle.

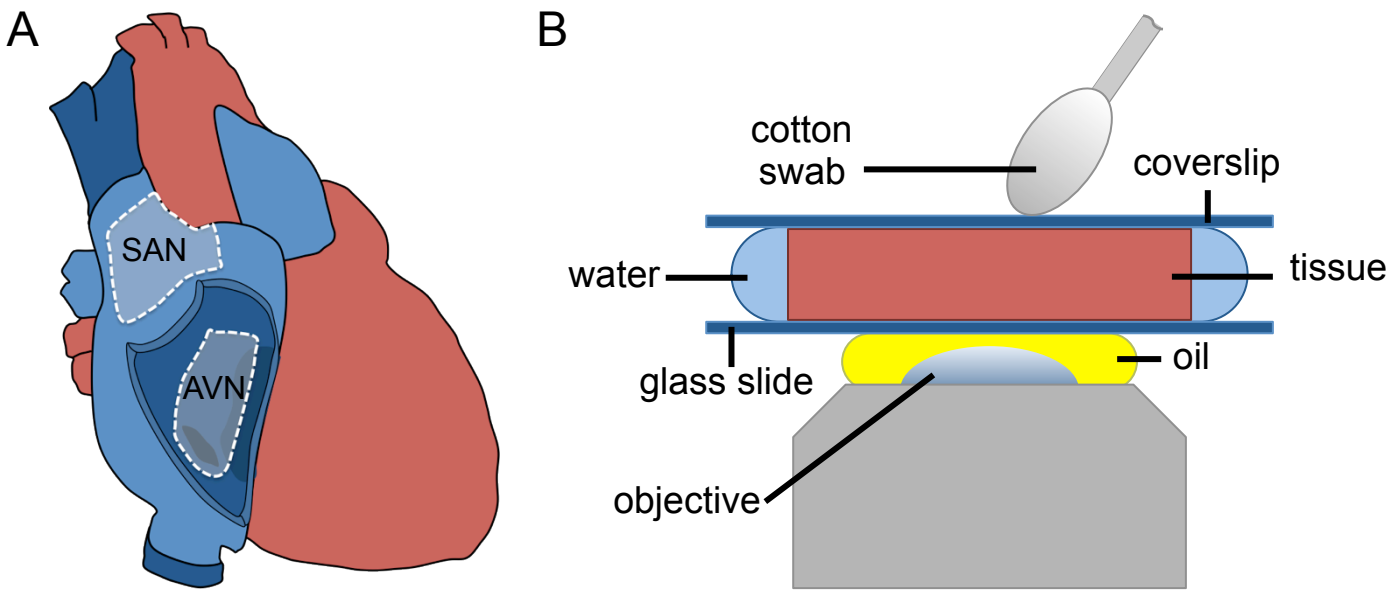

Supplemental Figure 2. Preparation and imaging of fixed cardiac tissue with conventional confocal microscopy. (**A**) Sketch of heart with SAN and AVN regions. Tissue preparations were excised from those regions after fixation of the heart. (**B**) Schematic of the imaging setup. Fluorescently labeled tissue was brought in close proximity to the glass slide for imaging.

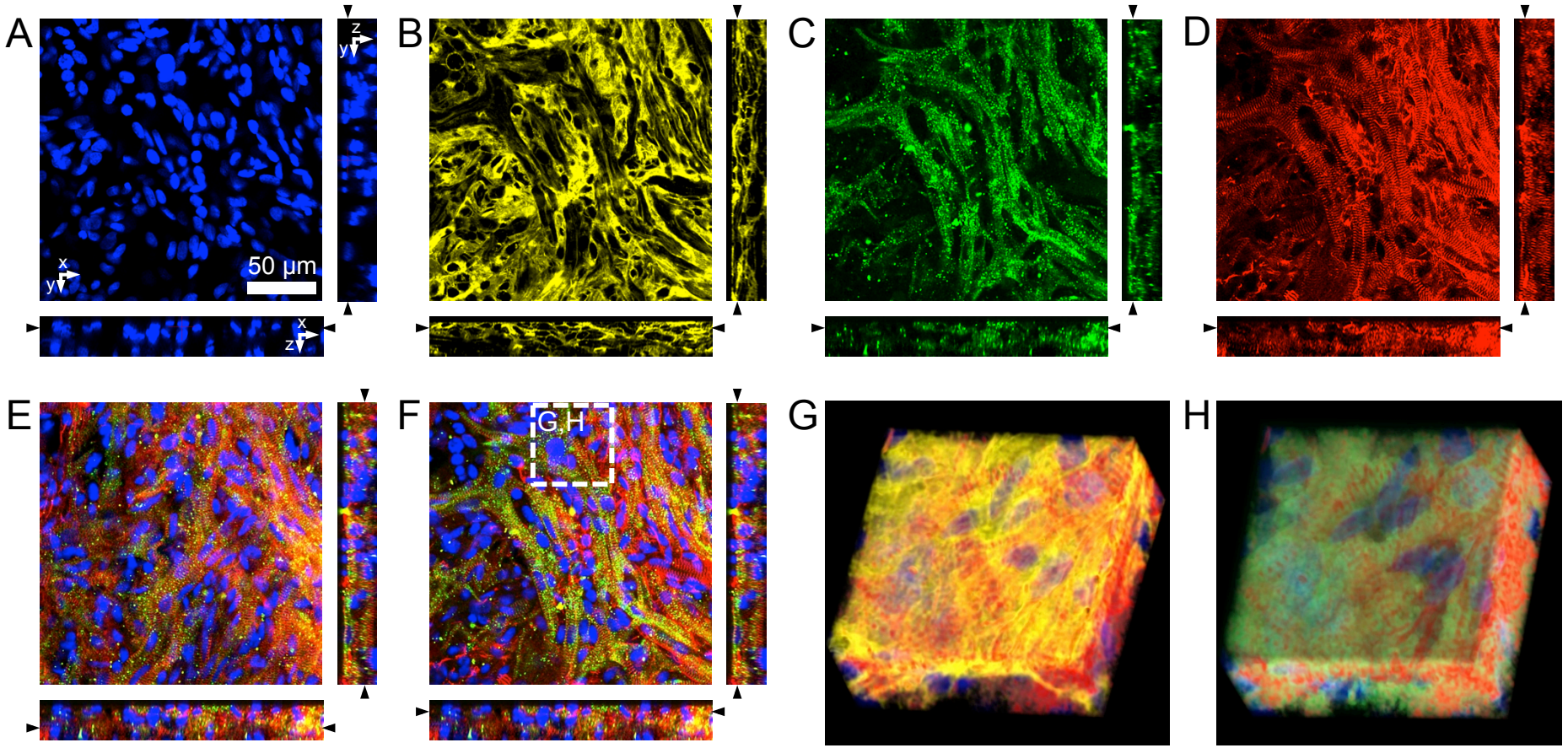

Supplemental Figure 3. Confocal microscopic images of AVN tissue. The tissue was labeled with (**A**) DAPI, (**B**) WGA, (**C**) anti-HCN4, and (**D**) anti-sarcomeric α-actinin. Irregular arranged, HCN-4 positive myocytes were located beneath the epicardial layer. An overlay of DAPI, anti-HCN4, anti-sarcomeric α-actinin images illustrates the irregular arrangement of myocytes located (**E**) at a depth of 16.2 µm and (**F**) beneath the epicardial layer. (**G**) Three-dimensional reconstruction of the region marked in (**F**) labeled with DAPI, WGA, and anti-sarcomeric α-actinin. (**H**) Three-dimensional reconstruction of the region marked in (**F**) after removal of the endocardial layer reveal the complex arrangement of AVN tissue. Scale bar in (**A**) applies to (**B-F**).

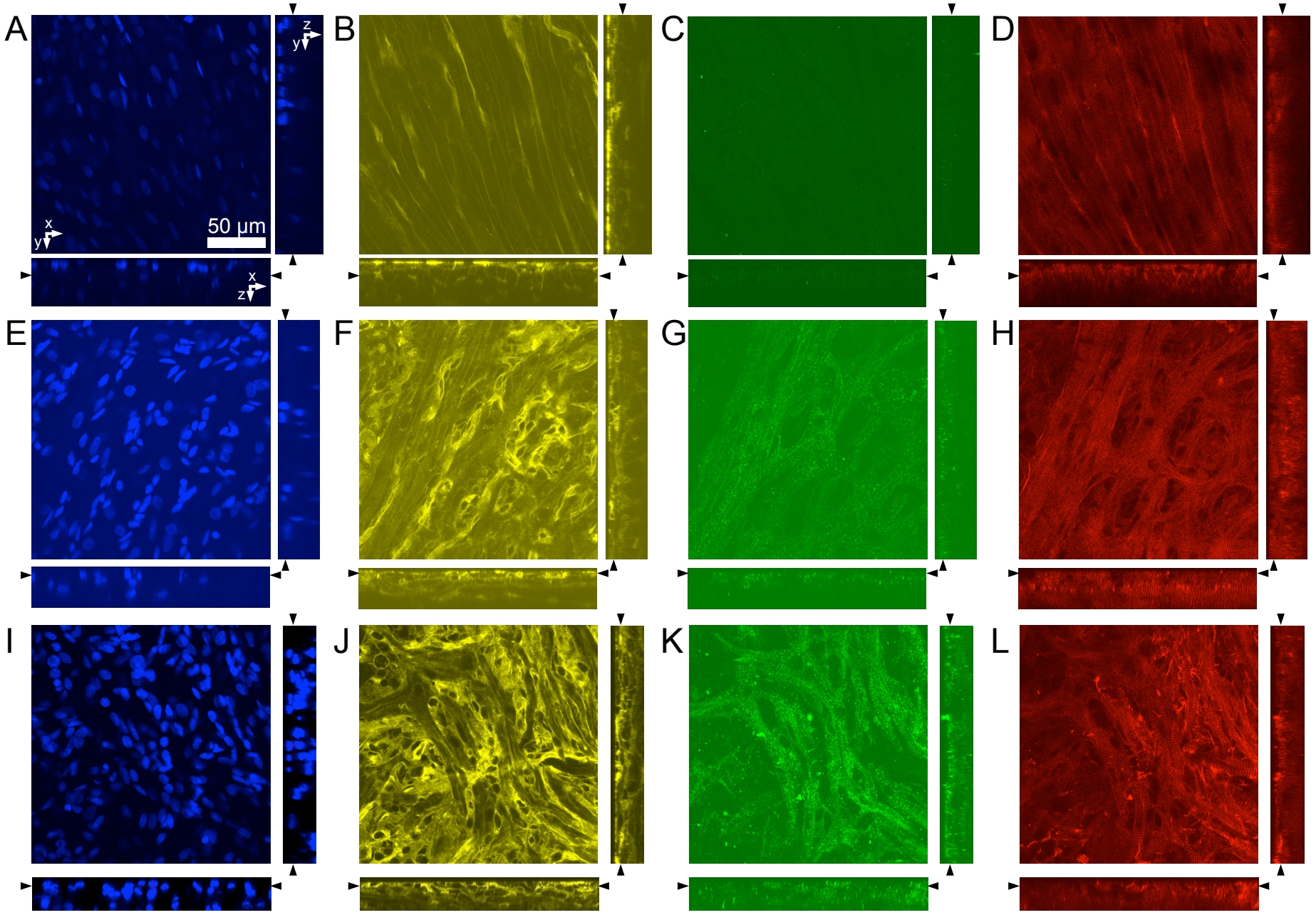

Supplemental Figure 4. Unprocessed images acquired with conventional confocal microscopy. Cross-sections through unprocessed image stacks corresponding to those presented in (**A-D**) Figure 2, (**E-H**) Figure 3, and (**I-L**) Supplemental Figure 3.

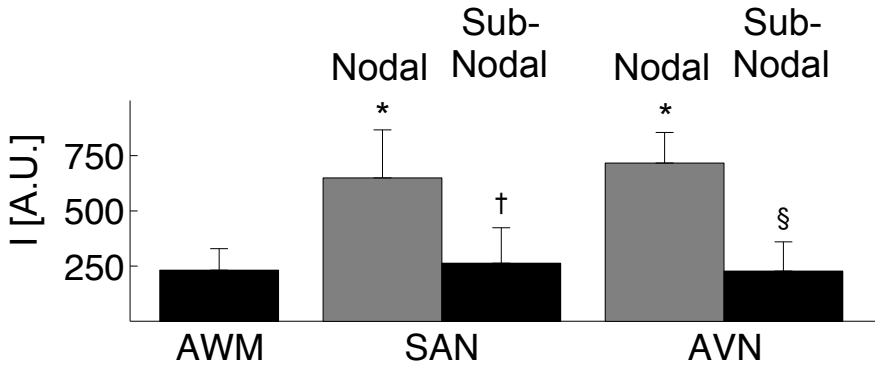

Supplemental Figure 5. Quantitative analysis of HCN4 signal intensity in AWM (*n* = 7/4), SAN (*n* = 5/4), and AVN (*n* = 6/3) tissue. The HCN4 signal in the SAN region was approximately 2.5 times higher in the nodal layer as compared to its subnodal layer. We found that the HCN4 intensity in the nodal layer of the AVN region was 3.1 times higher than its subnodal layer. The HCN4 level in the nodal layers of the SAN and AVN regions were 2.8 and 3.1 times higher respectively as compared to the HCN4 level in the AWM region. **P* < 0.005, compared with AWM. †*P* < 0.005, compared with SAN nodal layer. §*P* < 0.005, compared with AVN nodal layer. Sample size *n* is denoted as *n* = *I/A* where *I* = images and *A* = animals.

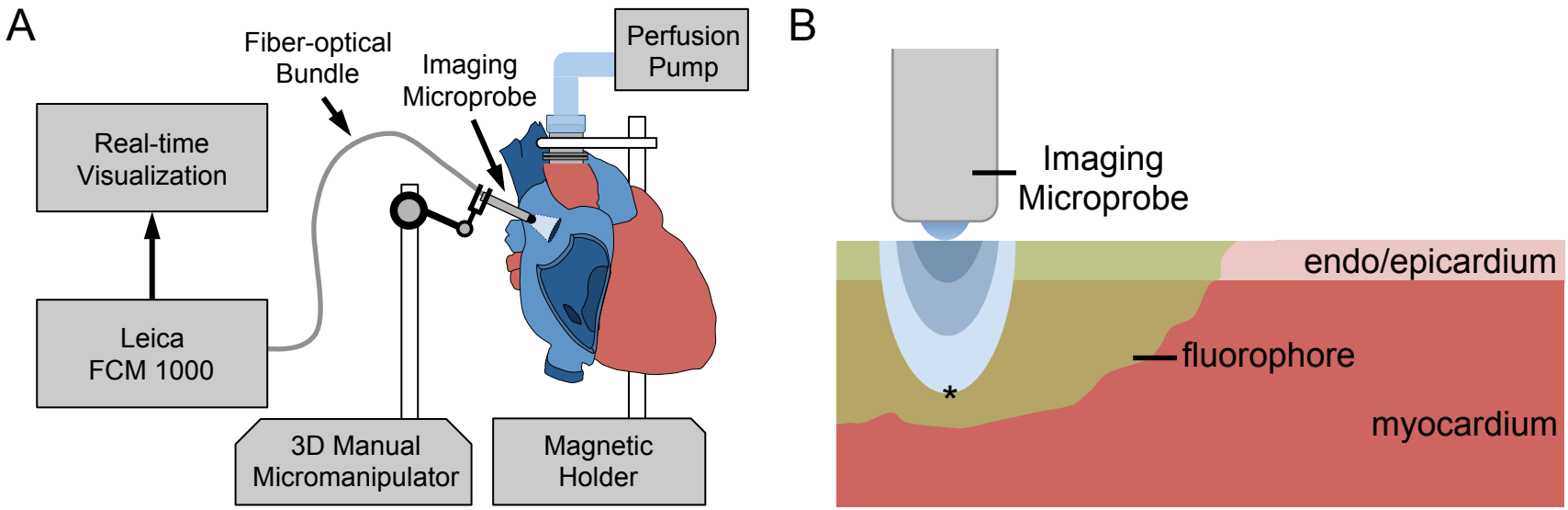

Supplemental Figure 6. Preparation and imaging of living cardiac tissue with FCM. (**A**) Setup for FCM imaging of living heart. The 3D manual micromanipulator is used to maneuver the imaging microprobe in close proximity to the epicardial or endocardial surface. (**B**) Illustration of imaging of 2-layered tissue. The fluorophore diffuses into the tissues after superficial application. The imaged region (*) is beneath a thin epicardial or endocardial tissue layer.

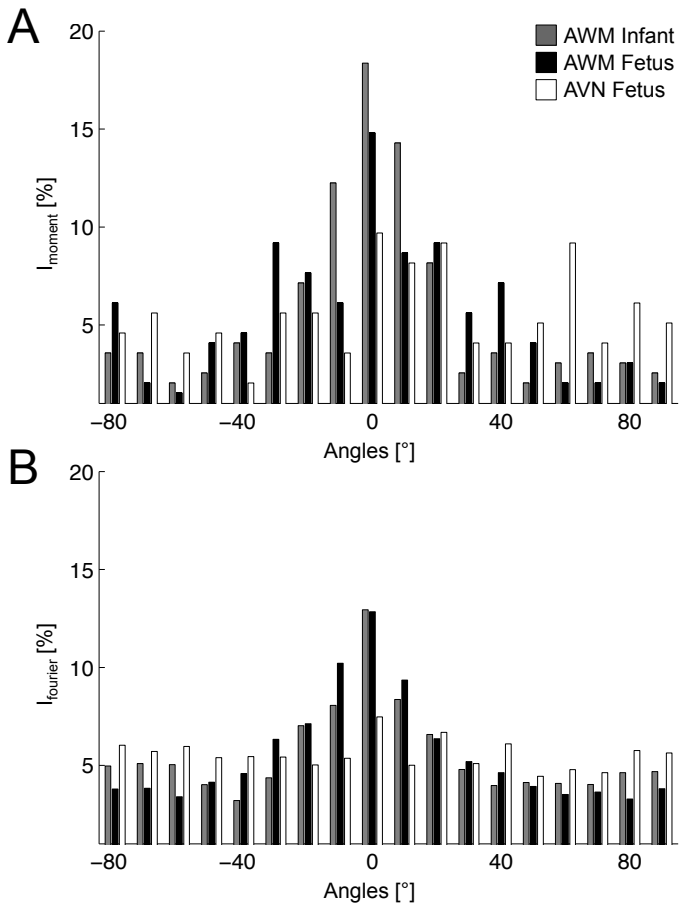

Supplemental Figure 7. Histogram of orientations based on (**A**) 2nd order image moments and (**B**) Fourier transforms of human AWM and AVN images shown in Figure 5.

Legends for Videos

Video 1. Real-time live imaging of rat AWM. The AWM tissue was labeled with dextran conjugated Alexa Fluor 488 and imaged using FCM. The dark regions shown are of muscle cells and the bright regions are of the fluorophore. The image sequence was taken at a rate of 20 images/s using a manual micromanipulator to maneuver the imaging microprobe in the region of interest.

Video 2. Real-time live imaging of rat SAN. The same imaging protocol used to acquire recordings in Video 7 was followed.

Video 3. Three-dimensional reconstruction of AWM. The tissue was imaged using conventional confocal microscopy. The 3D section has a field of view of (x) 118.9 μm, (y) 118.9 μm, and depth (z) 26.8 μm. Signals associated with DAPI, WGA, and sarcomeric α-actinin labeling are shown in blue, yellow, and red respectively.

Video 4. Three-dimensional reconstruction of AWM with epicardial layer removed. Signals associated with DAPI, WGA, and sarcomeric α-actinin labeling are shown in blue, yellow, and red respectively.

Video 5. Three-dimensional reconstruction of SAN. Reconstruction was performed from image stack acquired using conventional confocal microscopy with a field of view of (x) 118.9 μm, (y) 118.9 μm, and depth (z) 35.0 μm. Signals associated with DAPI, WGA, and sarcomeric α-actinin labeling are shown in blue, yellow, and red respectively.

Video 6. Three-dimensional reconstruction of SAN with endocardial layer removed. Signals associated with DAPI, HCN4, and sarcomeric α-actinin labeling are shown in blue, green, and red respectively.

Video 7. Three-dimensional reconstruction of AVN. Reconstruction was performed from image stack acquired using conventional confocal microscopy with a field of view of (x) 57.9 μm, (y) 57.9 μm, and depth (z) 28.4 μm. Signals associated with DAPI, WGA, and sarcomeric α-actinin labeling are shown in blue, yellow, and red respectively.

Video 8. Three-dimensional reconstruction of AVN with epicardial layer removed. Signals associated with DAPI, HCN4, and sarcomeric α-actinin labeling are shown in blue, green, and red respectively.